THE MICROSTRUCTURE INFLUENCE ON MECHANICAL PROPERTIES OF $Ti_{50}Ni_{50-x}Cu_x$ MATERIALS ACHIEVED BY SPARK PLASMA SINTERING AT 800°C–900°C

C.D. CIRSTEA[1,*], V. CIRSTEA[2], V. MARINESCU[1], D. PATROI[1], T.V. TIGANESCU[2]

[1] National Institute for Research and Development in Electrical Engineering INCDIE ICPE-CA, Romania
E-mails: diana_cirstea@yahoo.com, delia.patroi@icpe-ca.ro, virgil.marinescu@icpe-ca.ro
[2] Military Equipment and Technologies Research Agency, Romania
E-mails: vcirstea@acttm.ro, vtiganescu@acttm.ro
[*] *Corresponding author*: diana.cirstea@icpe-ca.ro

Received January 18, 2023

Abstract. The present study is focused on the understanding of the phenomenon and mechanism of phase transformations that were identified in $Ti_{50}Ni_{50-x}Cu_x$ materials after characterization of bulk materials realized from Ti, Ni and Cu powders using the spark plasma sintering technology between 800–900°C. The sintered materials with diameter of 20 mm and height of 4–5 mm were investigated by X-ray diffraction (XRD) and scanning electronic microscopy together with energy dispersive spectroscopy and nanoindentation measurements. The results of indentations are influenced by the existence of TiNiCu stable phases, Ti(Ni, Cu) phase precipitates, Ni or Ti unreacted observed in the microstructure of these materials, where the hardness value was about 350 HV and elastic modulus was about 75 GPa.

Key words: shape memory, spark plasma sintering, nanoindentation, phase precipitates.

1. INTRODUCTION

In metallic materials, intermetallic titanium/nickel/copper compounds are promising technological materials possessing many unique physical properties (*e.g.* hardness, acoustic absorption and high electric and thermal conductivity). Knowledge of the compounds and phases in the Ti-Ni-Cu ternary systems through the phase diagram is a necessary preliminary to a relevant experimental approach [1–5]. The NiTi binary system is composed of: a) solid solution of the pure element Ni, allotropic phase Ti with α-Ti and β-Ti and polymorphism TiNi phase corresponding to austenite phase (B2-cubic) for high temperature and martensite phase (B19-orthorhombic) and (B19'-monoclinic) for low temperature; b) and stoichiometric compounds $TiNi_2$, Ti_2Ni, $TiNi_3$, Ti_3Ni_4 metastable and polymorphism of Ti_2Ni_3 (orthorhombic at low temperatures and tetragonal at high temperatures) [1–3].

A similar behavior was found for phase relations in the constitutive Ti-Cu systems that are: a) the solid solutions of the pure components in stable form: α-Ti, β-Ti and Cu; b) the stoichiometric compounds Ti_2Cu, TiCu, Ti_3Cu_4, Ti_2Cu_3, $TiCu_2$ and $TiCu_3$ metastable crystalline phases with related crystal structures; c) and high- and low-temperature polymorphs β-$TiCu_4$ (stable phase) and α-$TiCu_4$ (metastable coherent phase at high temperature but stable at low temperature) [1, 3, 5].

The Ni-Cu phase diagram is composed of the liquid phase and the solid phase that is a stable and wide miscibility gap, which is not well established. In the region of the solid phase are large deviations that could be due to the slow kinetics in the low temperature region [2, 3].

Today, the technological progress is based on modern scientific and technological solutions, which result in modern high technology and new generation materials [2]. The production of metallic materials was possible through the use of powder technology procedures, where these procedures have been emerging to meet the challenge of conventional casting methods. Thus, the powder technology that uses the spark-plasma sintering (SPS) is one of the modern compaction methods. The SPS process is a complex technique that implies many processing parameters such as: sintering temperature, heating and cooling rates, maximum load, load/unload rate, with direct correlations between them [6, 7]. During the process of SPS, there is a competition between densification and grain growth because the removal of porosity depends on volume diffusion, while grain growth is controlled essentially by surface diffusion [6–9]. Also the heating/cooling rate can have a strong effect on the final microstructure of the material. Furthermore, the electric current pulses have an effect also on atomic diffusion, since high densities can be reached at very low temperatures and extremely short times as compared with classic sintering processes [7, 9–11].

In order to understand the temperature-controlled evolution of the studied alloys and associated mechanical properties, phase stabilities in the ternary system Ti-Ni-Cu are investigated.

2. MATERIALS AND METHODS

2.1. MATERIALS

For the manufacture of TiNiCu materials were used raw Ti, Ni and Cu materials in high purity powder form, acquired from Merck. Two different compositions ($Ti_{50}Ni_{45}Cu_5$ and $Ti_{50}Ni_{40}Cu_{10}$) were made by powder technology.

After the mixture of the powders, about 9 g were loaded into a graphite press mould with a diameter of 20 mm and placed into the chamber of the SPS installation. The parameters used for SPS are: uniaxial force pressing with 8 kN at

450°C for 120 seconds, holding with pressing for 240 seconds, heating at a temperature between 800°C to 900°C with pressing, holding for 120 seconds, cooling at 450°C with 160°C/min, holding for 120 seconds and cooling at room temperature in 120 seconds, in a regime of low-voltage pulses in on/off mode, in 12/2 bursts.

2.2. METHOD

The morphology and elemental composition of TiNiCu materials were investigated using a field emission FESEM-FIB scanning electron microscope Auriga type at ×500 magnification and at an acceleration voltage of 10 kV, equipped with energy dispersive spectrometry (EDS). The XRD investigation of our materials was performed with a X-ray source CuKα radiation (λ = 1.5406 Å) (Bruker, Germany), from 30° to 65°, with a 1D LynxEye detector and a scan step size of 0.5 s per step and 0.040° step size and Origin Pro software version 8.5.

The mechanical properties like Vikers hardness (HV) or Young Modulus (E_{IT}) were determined by nanoindentation tests, in accordance with the standards ISO 14577-1:2015 and ISO 14577-4:2016 for metallic materials [12, 13]. Five measurements were performed on each material and were conducted using CSM Instruments under the following conditions: the load was 500 mN with a Berkovich tip with α = 65.03°, the holding time was 30 s at F_{max}, the approach speed of the indenter was 4 μm/min and the loading/unloading rate was 20 N/min. The values of the mechanical properties were calculated by the Oliver and Pharr method, for Poisson's ration of 0.33 [12]. The indentation imprints were visualized by optical microscopy using a 50× objective attached to an Open Compact Platform.

3. RESULTS AND DISCUSSION

After pressing and sintering in SPS, the samples were noted with T_1, T_2 and T_3 for both composition $Ti_{50}Ni_{45}Cu_5$ and $Ti_{50}Ni_{40}Cu_{10}$, where T_1 is for 800°C, T_2 for 850°C and T_3 for 900°C, respectively. The TiNiCu samples presented a compact surface and a very good densification. Before SEM/EDS and XRD analysis, the materials were ground with silicon carbide paper from 320 up to 2400 grit size.

3.1. RESULTS OF SEM/EDS MEASUREMENTS

EDS elemental analysis on selected areas of $Ti_{50}Ni_{45}Cu_5$ sample has shown the existence of spectral lines corresponding to the constitutive and predominant phases of Titan (3.39–98.95 wt.%), Nickel (1.05–95.65 wt.%) and Cooper (0.0–3.40 wt.%). For the $Ti_{50}Ni_{40}Cu_{10}$ sample, spectral lines correspond to the constitutive Titan (1.21–98.59 wt.%), Nickel (1.09–74.56 wt.%) and Cooper

(0.32–27.16 wt.%). SEM/EDS results showed that the replacement of nickel up 10% of copper led to the formation of phases and compounds of Ti-Ni and less Ti-Cu or Ni-Cu.

Also, from SEM/EDS analysis for all samples (Figs. 1, 2, 3), we observed the surface diffusion of Ti or Ni in Ti_2(Ni, Cu) and (Ti, Cu)Ni_3 grain boundary and looks like islands that increase gradual from dark to grey zones. The diffusion phenomenon occurs due to the mass transport mechanism of the three constituent elements with different melting points (1668°C, 1455°C and 1085°C, respectively for Ti, Ni and Cu melting point), when a pressure is applied in the same time with sintering. For this reason, grain growth begins sooner than in traditional sintering where grain growth is slowed by porosity as a consequence Ti, Ni and Cu atoms move in response to the electric field formed after a DC electric current was applied to obtain the T_1, T_2 and T_3 sintering temperatures. Thus, it is difficult to clearly separate the effects of temperature, current and electric field. Some theories shown that the applied electric field and current increase conducted to a dominant mechanism like electromigration-diffusion in response based on the mobility or the concentration of defects at grain boundaries [9–11]. Some studies have reported [14] that higher cooling rates result in formation of Ti_2(Ni, Cu) or (Ti, Cu)Ni_3 precipitate phases in TiNiCu matrix phase and contains significant volume fraction of austenite/ martensite phase at room temperature. The existence of Ti_2(Ni, Cu) or (Ti, Cu)Ni_3 precipitate it is considered a defect in material, but also if the quantities are not too much they can contribute to the hardening of the material.

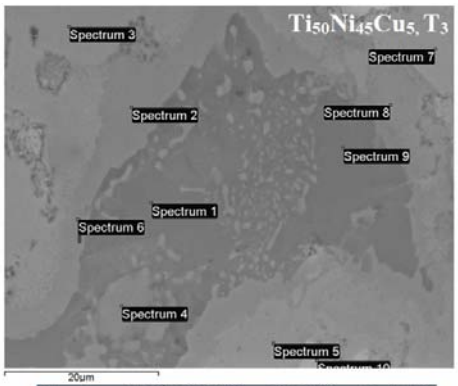

Spectrum EDX	Ti [wt%]	Ni [wt%]	Cu [wt%]
Spectrum 1	97.61	1.43	0.97
Spectrum 2	62.04	36.47	1.48
Spectrum 3	46.54	51.44	2.03
Spectrum 4	74.28	23.84	1.89
Spectrum 5	47.19	51.09	1.73
Spectrum 6	68.03	30.62	1.34
Spectrum 7	23.30	73.65	3.06
Spectrum 8	48.13	49.94	1.93
Spectrum 9	98.95	1.05	0.00
Spectrum 10	42.96	54.99	2.03

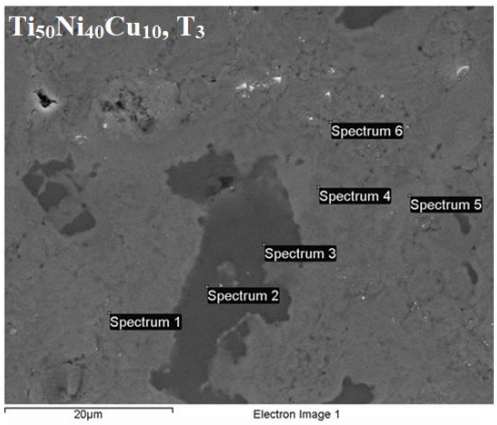

Spectrum EDS	Ti [wt%]	Ni [wt%]	Cu [wt%]
Spectrum 1	45.85	43.16	10.99
Spectrum 2	96.76	2.46	0.79
Spectrum 3	98.59	1.09	0.32
Spectrum 4	59.08	32.22	8.70
Spectrum 5	45.38	37.15	17.46
Spectrum 6	38.45	36.65	24.89

Fig. 1 – SEM/EDS results for TiNiCu, T_3 samples.

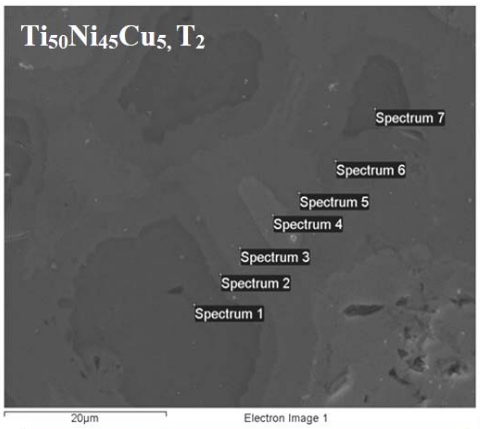

Spectrum EDX	Ti [wt%]	Ni [wt%]	Cu [wt%]
Spectrum 1	89.03	7.57	3.40
Spectrum 2	64.24	33.57	2.19
Spectrum 3	46.26	51.95	1.79
Spectrum 4	21.78	76.80	1.42
Spectrum 5	47.31	51.84	0.85
Spectrum 6	63.44	35.08	1.49
Spectrum 7	90.16	7.51	2.33

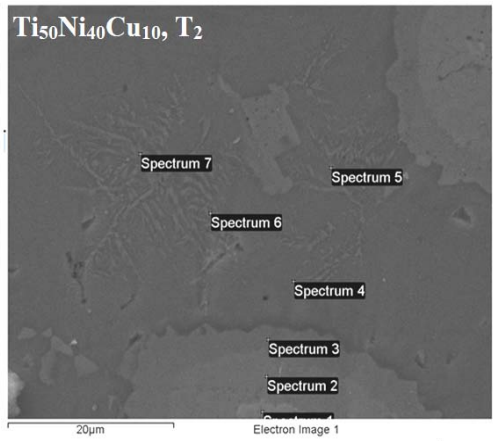

Spectrum EDX	Ti [wt%]	Ni [wt%]	Cu [wt%]
Spectrum 1	21.55	76.22	2.23
Spectrum 2	46.54	51.77	1.70
Spectrum 3	62.45	33.87	3.68
Spectrum 4	86.24	8.26	5.50
Spectrum 5	82.56	10.33	7.10
Spectrum 6	83.01	10.38	6.61
Spectrum 7	78.87	12.49	8.65

Fig. 2 – SEM/EDS results for TiNiCu, T_2 samples.

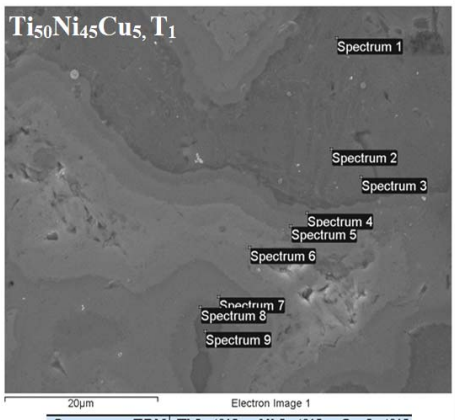

Spectrum EDX	Ti [wt%]	Ni [wt%]	Cu [wt%]
Spectrum 1	91.17	7.52	1.32
Spectrum 2	91.40	6.66	1.94
Spectrum 3	90.32	7.05	2.63
Spectrum 4	62.27	36.37	1.36
Spectrum 5	46.41	53.12	0.48
Spectrum 6	3.39	95.65	0.96
Spectrum 7	46.34	52.67	0.99
Spectrum 8	58.36	40.50	1.14
Spectrum 9	89.27	9.18	1.55

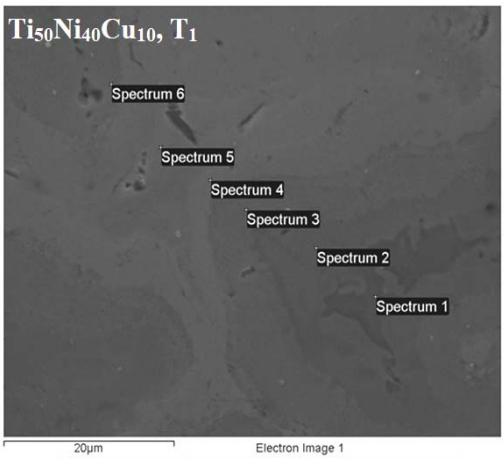

Spectrum EDX	Ti [wt%]	Ni [wt%]	Cu [wt%]
Spectrum 1	82.48	9.73	7.80
Spectrum 2	61.99	31.72	6.29
Spectrum 3	45.04	39.40	15.56
Spectrum 4	21.68	74.56	3.77
Spectrum 5	1.21	71.62	27.16
Spectrum 6	42.49	55.03	2.48

Fig. 3 – SEM/EDS results for TiNiCu, T_1 samples.

3.2. RESULTS OF XRD MEASUREMENTS

The crystalline structure of TiNiCu samples was analyzed through X-ray diffraction (Fig. 4). The crystalline phase identification from the XRD pattern was being done using the ICDD PDF 2 database. The recorded peaks reveal the presence of the following constituents: Ti, Ni, B2(TiNiCu), B19'(TiNiCu), B19(TiNiCu), Ti_2(Ni, Cu), (Ti, Cu)Ni_3 and (Ti, Cu)Ni_2. These results are in good, qualitative agreement with the EDS findings presented previously.

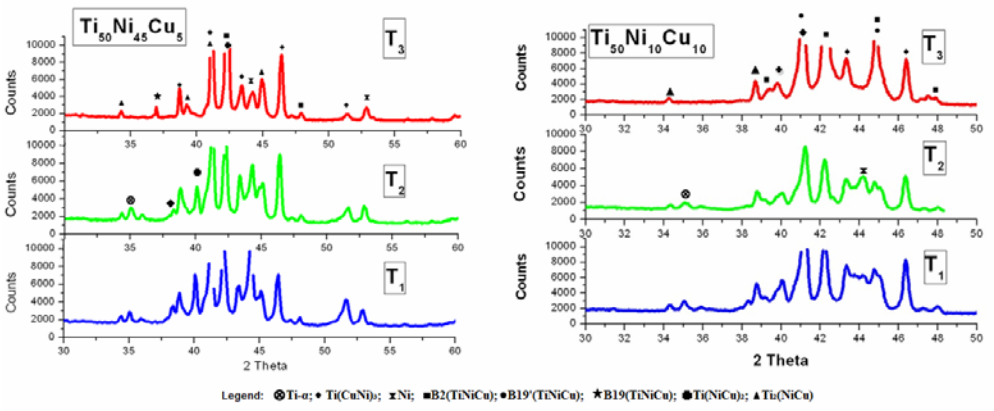

Fig. 4 – Difractogram for $Ti_{50}Ni_{45}Cu_5$ and $Ti_{50}Ni_{40}Cu_{10}$ samples.

Also, in X-ray diffraction spectra were searched some oxides, especially titanium ones and the Ti_2(Ni, Cu) that have the same crystal structure like Ti_4ONi_2. As it can be seen both from EDS analysis and diffraction spectrum, there were not identified such compounds or a line for Oxygen. If we compare microstructures from EDS and phase compositions – mainly amount and morphology of the Ti_2(Ni, Cu) phase from XRD with the same chemical compositions alloys prepared by powder metallurgy methods, there are some similarities and some differences. There are not so big differences in phase composition, but minor amount of residual nickel or titanium can remain after sintering reaction at 900°C (T_3).

Also, by increasing the sintering temperatures from T_1 (800°C) to T_3 (900°C), the XRD results for all samples show a progressively decreasing of Ti or Ni phases and increasing of Ti_2(Ni, Cu), TiNiCu or (Ti, Cu)Ni_3 phases. This results are in accordance with the reference [15], where the XRD test shows that the TiNiCu samples sintered consist of three phases at room temperature at 900°C: B19'(TiNiCu) monoclinic phase, B2(TiNiCu) cubic phase and (Ti, Cu)Ni_3 hexagonal phase. The more information about crystal structure is presented in Table 1.

Table 1

Crystallographic information for known crystal structures [1, 3]

Phase name	Crystal system	Space group	Lattice parameters (Å)
B2(TiNiCu)	Cubic	Pm-3m (221)	a = 3.015, α = β = γ = 90°
B19'(TiNiCu)	Monoclinic	P11121/m (11)	a = 2.8899, b = 4.1334, c = 4.6321, α = β = 90°, γ = 96.929°
B19 (TiNiCu)	Orthorhombic	Pmmb (51)	a = 2.919, b = 4.288, c = 4.5 α = β = γ = 90°
Ti-α	Hexagonal	P63/mmc (194)	a = 2.9486, c = 4.67, α = β = γ = 120°
Ni	Cubic	Fm-3m (225)	a = 3.586, α = β = γ = 90°
(Ti Cu)Ni_3	Hexagonal	P63/mmc (194)	a = 5.109, c = 8.299, α = β = γ = 20°
(Ti, Cu)Ni_2	Hexagonal	R-3m (166)	a = 2.549, c = 43,648, α = β = γ = 120°
Ti_2(Ni Cu)	Cubic	Fd-3m (227)	a = 11.3193, α = β = γ = 90°

Some studies [3, 4] shown that many Ti(Ni, Cu)$_2$ precipitates also exist in the interior of the B19' structure. However, some researchers reported the existence of B19' martensite in the Ti–Ni–Cu thin films with high Cu content (>15%) on the basis of the internal friction measurements without the TEM observations [16–18].

Another phase identified by XRD is (Ti, Cu)Ni_3 precipitate. The (Ti, Cu)Ni_3 lattice evolution is found inducing converse lattice shrinkage and expansion in *B2* (TiNiCu) lattice during the dissolution and precipitation of $TiNi_3$, respectively [17, 19, 20]. T. Goryczka *et al.* [19] considered that alloys with low-content of Cu (< 10%at), have a nontransformable phase (Ti, Cu)Ni_3, which shows the same type of crystal structure as the Cu_3Ti phase occurs but in our measurements this structure corresponds to the $TiNi_3$ phase.

3.3. RESULTS OF NANOINDENTATION MEASUREMENTS

The mean ($F_n - P_d$) force-displacement curves for all the TiNiCu samples on each flat circular surface, together with optical images of some residual imprints for T_3 are shown in Fig. 5. The elastic properties are determined by Oliver&Pharr methods from the unloading portion of the ($F_n - P_d$) curve [21]. This curve is described by a power law ($F = CP_d^2$, where C can be determined for a sharp Berkovich indenter) that relates the unloading load to the indentation depth, and the slope at the peak load is obtained by analytical differentiation of this relation.

The indentation modulus, E_{IT} [GPa] that represents the elastic modulus of the sample was calculated from the equation (1) [12] using an estimated Poisson's ratio of TiNiCu samples (υ_2) of 0.33:

$$E_{IT} = E^* \cdot (1 - \vartheta_2^2) \tag{1}$$

with

$$E^* = \left(\frac{1 - \vartheta_1^2}{E_1} + \frac{1 - \vartheta_2^2}{E_2} \right) \tag{2}$$

with E^* representing a reduced modulus that accounts for non-rigid indenters. E_1 and ν_1 represent the elastic modulus and the Poisson's ratio of the indenter, respectively, while E_2 and ν_2 represent the elastic modulus and Poisson's ratio of the indented TiNiCu samples, respectively.

In Fig. 5, the hardness of the samples increases with the increase of the sintering temperature, but not too much when increasing the content of Cu in TiNiCu materials. The established microhardness of samples achieved by SPS is at the level of 282–445 HV for $Ti_{50}Ni_{40}Cu_{10}$ and 335–363 HV for $Ti_{50}Ni_{45}Cu_5$, with increasing temperature from T_1 to T_3. Although the hardness increases only slightly, in both materials compositions, there are variations of the average, which indicates the presence of multiphase identified by our XRD measurements. Vickers hardness measurements is a good indicator of hardness for non-ferrous alloys (values usually up to 320 HV) [2, 22, 23]. Based on the results of the images of the sample, one can judge the sufficient plasticity of the sample.

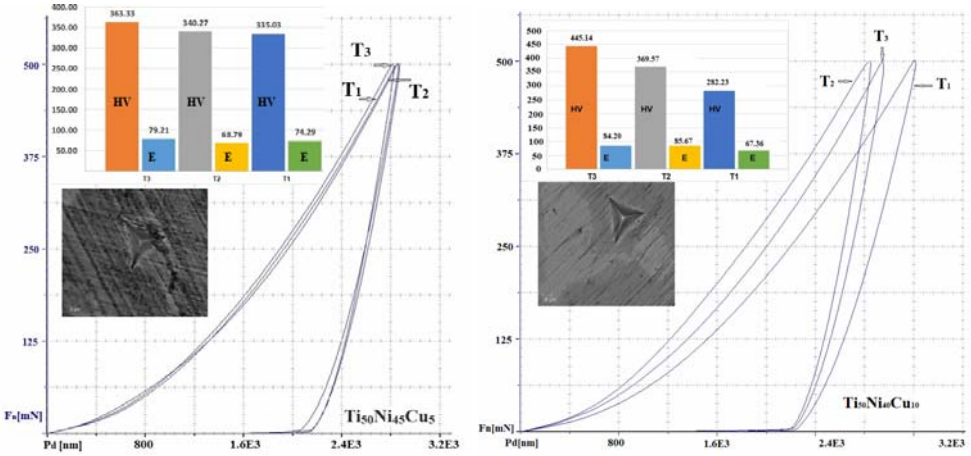

Fig. 5 – Vickers hardness and Young's modulus values of the NiTiCu samples.

The Young's modulus determined between 74–79 GPa for $Ti_{50}Ni_{45}Cu_5$ and 67–84 GPa for $Ti_{50}Ni_{40}Cu_{10}$ suggests that the materials are located at the lower limit of the austenitic type materials [19].

Table 2

Microhardness and Young Module values for materials obtained by spark plasma sintering

$Ti_{50}Ni_{45}Cu_5$						
	T_1 = 800°C		T_2 = 850°C		T_3 = 900°C	
	HV	E_{it} (GPa)	HV	E_{it} (GPa)	HV	E_{it} (GPa)
	320.918	72.184	367.38	65.513	336.657	75.694
	381.399	78.065	330.211	73.823	367.464	85.539
	308.897	74.982	306.184	67.189	374.672	83.502
	289.364	68.877	341.526	66.134	388.421	73.557
	374.58	77.354	356.056	71.271	349.436	77.777
Med ± std. dev	335.03 ± 36.56	74.29 ± 3.40	340.27 ± 23.71	68.79 ± 3.60	363.33 ± 18.33	79.21 ± 4.58
$Ti_{50}Ni_{40}Cu_{10}$						
	T_1 = 800°C		T_2 = 850°C		T_3 = 900°C	
	HV	E_{it} (GPa)	HV	E_{it} (GPa)	HV	E_{it} (GPa)
	278.275	64.801	381.24	83.21	438.752	82.503
	281.36	71.618	363.94	83.99	474.867	87.033
	291.368	71.705	383.05	93.21	447.28	81.688
	277.46	65.735	366.42	89.17	411.586	83.932
	282.682	62.922	353.21	78.75	453.203	85.826
Med ± std. dev	282.23 ± 5.54	67.36 ± 4.06	369.57 ± 12.52	85.67 ± 5.61	445.14 ± 23.02	84.20 ± 2.23

4. CONCLUSIONS

This paper aims to present the results obtained for a TiNiCu-based alloy made by the SPS method and demonstrates the hardening potential of multi-phase TiNiCu alloys due to the formation of ternary titanium-nickel-copper compounds. Also extremely rapid temperature increase and high cooling rates can be attributed to the crystallization of Ti_2(Ni, Cu) and (Ti, Cu)Ni_3 intemetallic compound in TiNiCu matrix.

From the analysis of the results obtained from the mechanical indentation of the studied samples, it is observed that they are influenced by the existence of both stable TiNiCu, Ni or Ti phases and the existence of (Ti(Ni, Cu)$_2$) phase precipitates observed in the microstructure of these materials.

The hardness value was about 350 HV and the elastic modulus was about 75 GPa. The good mechanical properties of the multiphase alloys obtained in this work suggest the idea of further investigations.

Acknowledgements. This work was supported by the Romanian Ministry of Research, Innovation and Digitalization, project number 25PFE/30.12.2021-Increasing R-D-I capacity for electrical engineering-specific materials and equipment with reference to electromobility and "green" technologies within PNCDI III, Programme 1, project no. PN19310102/2019 – Advanced metallic and micro/nanostructured composite materials with high performance properties for practical applications in priority areas, under the contract no. 46N/2019 and Bilateral Collaboration Roumania – JINR under the Project No. 62/2016 (JINR Orders 95 and 96/15.02.2016).

REFERENCES

1. K. P. Gupta, *The Cu-Ni-Ti (Copper-Nickel-Titanium) System, Phase Diagram Evaluation*, Section II, Journal of Phase Equilibria **23** (6), 541–547 (2002).
2. O. O. Shichalin *et al*., *Synthesis of Ti-Cu multiphase alloy by spark plasma sintering: mechanical and corrosion properties*, Metals **12**, 1089 (2022).
3. X. L. Meng *et al.*, *Structure of martensite in sputter-deposited (Ni, Cu)-rich Ti-Ni-Cu thin films containing Ti(Ni, Cu)$_2$ precipitates*, Acta Materialia **57**, 1525–1535 (2009).
4. J.-h. Kim, J.-h. Lim, J. G. Kim *et al.*, *Microstructure, transformation behavior and superelasticity of an aged Ti-40Ni-12Cu (at%) shape memory alloy*, Journal of Alloys and Compounds **900**, 163390 (2022).
5. J. C. Schuster, G. Cacciamani, *Cu-Ni-Ti (Copper – Nickel – Titanium)*, Stuttgart, 2006.
6. T. H. Nam, S. G. Hur, I. S. Ahn, *Phase transformation behaviours of Ti-Ni-Cu shape memory alloy powders fabricated by mechanical alloying*, Met. Mater. Int. **4**, 61–66 (1998), doi:10.1007/ BF03026066.
7. Z. A. Munir, U. Anselmi-Tamburini, *The effect of electric field and pressure on the synthesis and consolidation of materials: A review of the spark plasma sintering method*, Journal of Materials Science **41**, 763–777 (2006).
8. S. H. Kang, S. G. Hur, H. W. Lee, T. H. Nam, *Microstructures and transformation behavior of Ti-Ni-Cu shape memory alloy powders fabricated by ball milling method*, Met. Mater. Int. **6**, 381–387 (2000), doi:10.1007/BF03028086.
9. R. Orru, R. Licheri, A. M. Locci, A. Cincotti, G. Cao, *Consolidation/synthesis of materials by electric current activated/assisted sintering*, Mat. Sci. Eng. R **63**, 127– 287 (2009).
10. J. Garay, S. Glade, U. Anselmi-Tamburini, P. Asoka-Kumar, Z. Munir, *Electric current enhanced defect mobility in Ni$_3$Ti intermetallics*, Applied Physics Letters **85** (4), 573–575 (2004).
11. Matthew Thomas Luke, *Microstructural Evolution of Nickel During Spark Plasma Sintering*, PhD Thesis, 2010.
12. ISO 14577-1, Metallic materials – Instrumented indentation test for hardness and materials parameters – Part 1: Test method, 2015.
13. ISO 14577-4, Metallic materials – Instrumented indentation test for hardness and materials parameters – Part 4: Test method for metallic and non-metallic coatings, 2016.
14. C. D. Cirstea *et al.*, *Phase relation in the NiTiCu shape memory materials used in medicine applications*, Rev. Roum. Chim. **62** (6–7), 539–544 (2017).
15. A. A. Atiyah, A-R. K. A. Ali, N. M. Dawood, *Characterization of NiTi and NiTiCu Porous Shape Memory Alloys Prepared by Powder Metallurgy (Part I)*, Materials Science, Arabian Journal for Science and Engineering, March 2015, DOI:10.1007/S13369-014-1538-0, Corpus ID: 137336619.
16. J. X. Zhang, M. Sato, A. Ishida, *Structure of martensite in sputter-deposited Ti–Ni thin films containing Guinier–Preston zones*, Acta Mater **49**, 3001–3010 (2001).
17. T. Goryczka, M. Karolus, P. Pchin, H. Morawiec, J. Phys., IV France **11**, 345 (2001).
18. I. Yoshida, D. Monma, K. Iino, K. Otsuka, M. Asai, H. Tsuzuki, *Damping properties of Ti50Ni50–xCux alloys utilizing martensitic transformation*, J. Alloys Compd. **355**, 79–84 (2003).
19. T. Goryczka, J. Van Humbeeck, *Characterization of a NiTiCu shape memory alloy produced by powder technology*, Journal of Achievements in Materials and Manufacturing Engineering **17** (1–2), (2006).
20. F. J. J. Van Loo, G. F. Bastin, A. J. H. Leenen, *Phase relations in the ternary Ti-Ni-Cu system at 800 and 870°C*, Journal of the Less-Common Metals **57** (1), 111–121 (1978). https://doi.org/ 10.1016/0022-5088(78)90167-4.
21. Sudhir Rajagopalan, *Instrumented Nanoindentation Studies of Deformation in Shape Memory Alloys*, Electronic Thesis and Dissertations, University of Central Florida, 2005.
22. N. Poondla, T.S. Srivatsan, A. Patnaik, M. Petraroli, *A study of the microstructure and hardness of two titanium alloys: Commercially pure and Ti-6Al-4V*, J. Alloys Comp. **486**, 162–167 (2009).
23. K.S. Chenna, A.J. Jha, P. Bhanu, *On prediction of strength from hardness for cooper alloys*, J. Mater **2013**, 352578 (2013).